

1 **A physics-based universal indicator for vertical**
2 **decoupling and mixing across canopies architectures**
3 **and dynamic stabilities**

4 **O. Peltola¹, K. Lapo^{2,3}, C. K. Thomas^{2,3}**

5 ¹Climate Research Programme, Finnish Meteorological Institute, P.O. Box 503, 00101 Helsinki, Finland

6 ²Micrometeorology Group, University of Bayreuth, Bayreuth, Germany

7 ³Bayreuth Center for Ecology and Environmental Research, Bayceer, University of Bayreuth, Bayreuth,
8 Germany

9 **Key Points:**

- 10 • a universal indicator for air flow vertical decoupling is derived
11 • the indicator enables analytical estimation of flow decoupling dependency on height,
12 stratification and leaf area index
13 • the indicator should be applicable at most flux measurement sites, since it relies
14 only on basic micrometeorological measurements

Corresponding author: O. Peltola, olli.peltola@fmi.fi

Abstract

Air flows may be decoupled from the underlying surface either due to strong stratification of air or due to canopy drag suppressing cross-canopy mixing. During decoupling, turbulent fluxes vary with height and hence identification of decoupled periods is crucial for the estimation of surface fluxes with the eddy-covariance (EC) technique and computation of ecosystem-scale carbon, heat, and water budgets. A new indicator for identifying the decoupled periods is derived using forces (buoyancy and canopy drag) hindering movement of a downward propagating air parcel. This approach improves over the existing methods since 1) changes in forces hindering the coupling are accounted for and 2) it is based on first principles and not on ad-hoc empirical correlations. The applicability of the method is demonstrated at two contrasting EC sites (flat open terrain, boreal forest) and should be applicable also at other EC sites above diverse ecosystems (from grasslands to dense forests).

Plain Language Summary

Air flows may be disconnected (i.e. decoupled) from the surface below, meaning that the properties of the flow (e.g. wind speed, temperature, concentrations of gases, pollutants or particles) do not react to changes at the surface. During these periods, air temperatures near the ground decrease and concentrations of gases, pollutants and particles increase significantly since they are not transported upwards, but rather stay close to the ground. These decoupling periods can take place when the air is strongly stratified (e.g. clear-sky, weak wind nights) or thick forest canopies inhibit air mixing. Controls on flow decoupling are poorly understood, yet the phenomenon has significance for scientific monitoring networks and also for the general public due to its connection e.g. to air quality and frost formation. In this study, we derive a new indicator for flow decoupling, demonstrate its applicability at two measurement sites and discuss variables controlling decoupling in the light of this new indicator.

1 Introduction

Understanding of air flows and mixing in the very stable boundary layer (vSBL) often observed e.g. during clear-sky, weak wind nights persists to be incomplete (Mahrt, 2014). This issue poses problems for all scientific studies enquiring into surface-atmosphere interactions including mass and energy budgets, since they rely on turbulence observations or boundary-layer theories, both of which tend to fail under strong stratification.

The stable stratification, resulting from surface cooling via radiative heat loss, suppresses vertical turbulent mixing. Under strong enough stratification and weak turbulence production via wind shear, the turbulent eddies become detached from the surface, i.e. they are not coupled to the surface. This results in so-called "z-less" scaling of turbulence statistics (Nieuwstadt, 1984), meaning that distance from the surface is no longer a governing length scale (Sorbjan, 2006; Sorbjan & Balsley, 2008; Grachev et al., 2013; Li et al., 2016). As eddies detach from the surface, they lose their immediate connection to the exchange of momentum, heat and gases at the surface resulting in vertical variability of turbulent flux of these constituents with height (Mahrt et al., 2018).

Vertical variability of turbulent flux in this decoupled flow regime poses a severe problem for the global eddy covariance (EC) flux measurement network (FLUXNET) (Baldocchi, 2014) and a clear solution for the problem is lacking (Aubinet et al., 2010). FLUXNET is the main observational tool to study global terrestrial carbon and water cycles and the accuracy of the network largely hinges upon proper identification of decoupled and coupled flow regimes. Only in latter case EC observations integrate over all sinks and sources and thus can provide biophysically meaningful estimates of carbon, wa-

63 ter and heat budgets. Accurate estimates of terrestrial carbon cycle are sorely needed
64 for constraining the global carbon budget (Friedlingstein et al., 2019).

65 Commonly the friction velocity (u_*) is used to identify decoupled periods from con-
66 tinuous flux time series, albeit this approach is known to be flawed, in particular at sites
67 with dense canopies (Acevedo et al., 2009; Thomas & Foken, 2007a; Thomas et al., 2013;
68 Jocher et al., 2018; Freundorfer et al., 2019). Various other metrics have been used to
69 identify the weakly stable from the very stable flow regime (Mahrt et al., 1998; Sun et
70 al., 2012; Williams et al., 2013). However, they all rely on uncertain site specific thresh-
71 old values and were developed for open areas and hence their applicability to forested
72 regions remains unclear (Freundorfer et al., 2019). Canopy flows differ markedly from
73 the air flows above short vegetation, due to prevalence of coherent flow structures (Raupach
74 et al., 1996; Finnigan, 2000; Thomas & Foken, 2007b; Finnigan et al., 2009) and the mo-
75 mentum sink for the air flow caused by canopy drag. The latter can cause the air flows
76 above forests to be decoupled from the forest floor also during daytime (Kruijt et al., 2000;
77 Thomas et al., 2013; Jocher et al., 2017, 2018; Santana et al., 2018).

78 In this study we aim to advance the mechanistic understanding of flow coupling
79 to the surface, in particular in the presence of emergent vegetation and/or strong strat-
80 ification. Here we define a 'weakly stable regime' to be governed by eddies which com-
81 municate with the surface (z -scaling applies), whereas in the 'strongly stable regime' the
82 large wall-attached eddies are not prevalent. A simple air parcel technique is used to eval-
83 uate the flow coupling to the surface. A novel metric is proposed to identify the flow regime
84 and variables controlling the decoupling are discussed. The metric may be applied across
85 the entire gradients from short canopies (e.g. grass, crop, snow) to dense tall forests and
86 hence applicable at most flux sites monitoring ecosystem-atmosphere interactions.

87 2 Theory

88 Coupled air layers are defined in this study as follows: air parcels travel between
89 the coupled air layers and facilitate the exchange of heat, mass and momentum between
90 the layers. Therefore there is a direct interaction between the layers. In contrast, air parcels
91 do not travel between decoupled air layers and hence there is no direct interaction be-
92 tween the layers (albeit waves can still transport momentum). When considering cou-
93 pling of air layer at height z above ground with the surface, based on this definition there
94 need to be air parcels that can traverse the vertical distance of z . This concurs with the
95 notion that in coupled situations large wall-attached eddies that scale with z dominate
96 the flow (Sun et al., 2012; Lan et al., 2018; Sun et al., 2020). Note that the concept pro-
97 posed below is based on first principles and does not assume e.g. the surface layer simi-
98 larity theories to be valid. Similar air parcel approaches have been used (e.g. Mahrt,
99 1979; Sorbjan, 2006; Sorbjan & Balsley, 2008; Mahrt et al., 2012; Zeeman et al., 2013)
100 to derive e.g. relevant length scales in the stable boundary layer, here it is used in canopy
101 flows to examine the coupled air layer.

102 Movement of downward moving air parcels at the canopy height (h) is hindered by
103 any opposing forces which include canopy drag caused by the foliage (e.g. Poggi, Katul,
104 & Albertson, 2004; Cescatti & Marcolla, 2004; Watanabe, 2004) and buoyancy force in-
105 flicted by stably stratified air layers. In order to reach the ground, an air parcels kinetic
106 energy must match or exceed the work performed against the hindering forces. Based
107 on this a critical speed ($w_{e,crit}$) for the air parcel can be derived (see supporting infor-
108 mation):

$$109 \quad w_{e,crit} = -\gamma \hat{c}_d \text{LAI} U_h - \sqrt{\gamma^2 \hat{c}_d^2 \text{LAI}^2 U_h^2 + 2gh \frac{\theta_e - \hat{\theta}}{\hat{\theta}}}, \quad (1)$$

110 where γ is a constant ($=0.277$) depending on the horizontal wind and downward pen-
111 etrating air parcel speed profiles below canopy height h (e.g. Inoue, 1963; Amiro, 1990a;
112 Poggi, Porporato, et al., 2004; Yi, 2008), \hat{c}_d is the mean drag coefficient below h (equal

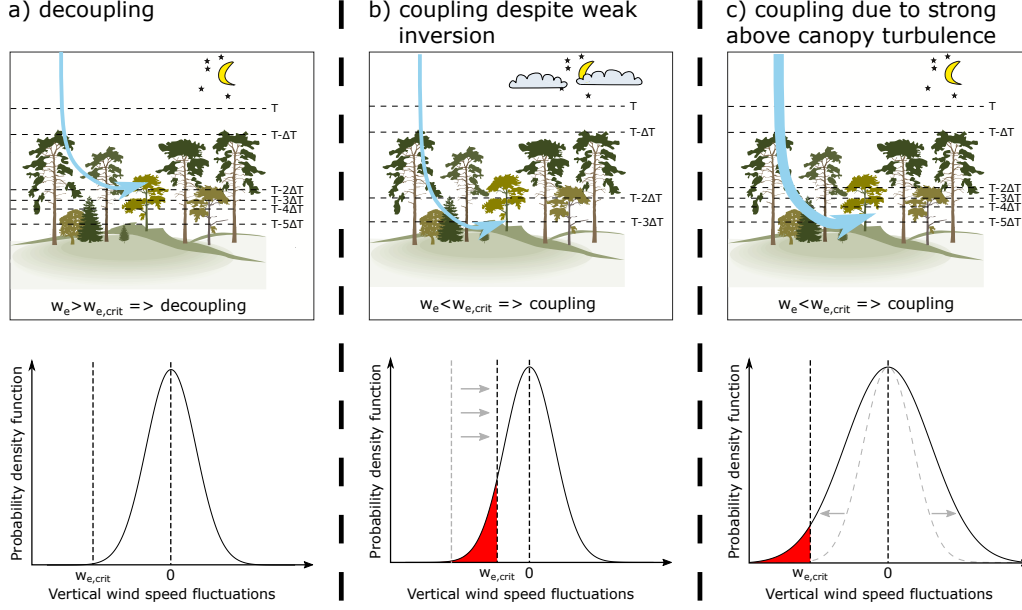


Figure 1. Schematic illustration of different decoupling situations. a): the above canopy flow is decoupled from the surface since the negative vertical wind speed fluctuations are not strong enough to counterbalance the movement hindering forces. b): coupling with the surface due to weaker stratification compared to a). c): coupling due to stronger turbulent fluctuations when compared to a). Bottom: fraction of w' data below $w_{e,crit}$ is shown with red.

113 to 0.15 for this study), LAI is leaf area index, U_h is horizontal wind speed at the canopy
 114 height (m s^{-1}), g is the acceleration due to gravity (m s^{-2}), $\hat{\theta}$ is the mean potential tem-
 115 perature below h and θ_e is the potential temperature of the downward moving air par-
 116 cel. If the speed of the air parcel is equal to $w_{e,crit}$, then its kinetic energy is sufficient
 117 to counterbalance the work performed against the hindering forces. However, if it is less
 118 than this critical speed, then its downward movement stops before it reaches the ground
 119 and as a result interaction with the surface does not occur (see Fig. 1).

120 In order to couple above canopy flow with the forest floor a large enough fraction
 121 of negative vertical wind speed fluctuations (w') needs to be below $w_{e,crit}$. Considering
 122 Taylor's frozen turbulence hypothesis, this coincides with the definition that in coupled
 123 flow large enough cross-sectional area of the flow at height z needs to be governed by strong
 124 downward gusts which interact with the surface. Here we defined the flow to be coupled
 125 with the surface when more than 5% of the w' data were below $w_{e,crit}$, weakly coupled
 126 when between 1% and 5% of w' data were below $w_{e,crit}$ and decoupled when less than
 127 1% were below $w_{e,crit}$. Future work is needed to validate the general applicability of these
 128 thresholds, yet their applicability at two contrasting sites are demonstrated below (see
 129 also Sect. 4.4). Assuming Gaussian distribution for w' , these criteria can be described
 130 using the standard deviation of w :

$$\begin{aligned}
 131 \quad & \Lambda \geq 0.61 \rightarrow \text{coupled} \\
 132 \quad & 0.43 \leq \Lambda < 0.61 \rightarrow \text{weakly coupled} \\
 133 \quad & \Lambda < 0.43 \rightarrow \text{decoupled}
 \end{aligned} \tag{2}$$

134 where the decoupling metric Λ is defined as $\frac{\sigma_w}{|w_{e,crit}|}$. Therefore the flow can couple with
 135 the ground if σ_w increases (turbulent mixing increases), U_h or LAI decrease (canopy drag
 136 decreases) or $(\theta_e - \hat{\theta})$ or h decreases (influence of buoyancy and vertical distance decrease).

137 Atmospheric observations are typically made at some distance above the canopy
 138 during which the speed of downward propagating air parcel may be already slowed down
 139 due to stratification. The change in the speed of the air parcel when it traverses between
 140 heights z and h can be calculated as

$$141 \quad w_e(z) = -\sqrt{w_e(h)^2 + 2g(z-h)\frac{\theta_e - \tilde{\theta}}{\tilde{\theta}}}, \quad (3)$$

142 where $w_e(z)$ and $w_e(h)$ are the air parcel speed at heights z and h and $\tilde{\theta}$ is the mean air
 143 potential temperature between z and h . Hence in order to evaluate the coupling of air
 144 at height z with the ground, Eq. 1 should be used to calculate $w_{e,crit}$ at the canopy height
 145 (h) and then use Eq. 3 to translate this value from h to z prior to comparing to σ_w val-
 146 ues at height z .

147 In the case of neutral stratification, $w_{e,crit}$ reduces to

$$148 \quad w_{e,crit} = -2\gamma\hat{c}_d\text{LAI}U_h, \quad (4)$$

149 indicating that the limiting vertical wind speed needed to couple with the forest floor
 150 increases linearly with LAI and U_h . On the other hand, in the case of flat surfaces with-
 151 out emergent vegetation (i.e. LAI \approx 0), $w_{e,crit}$ reduces to

$$152 \quad w_{e,crit} = -\sqrt{2gz\frac{\theta_e - \hat{\theta}}{\hat{\theta}}} = -\sqrt{2}zN, \quad (5)$$

153 where N is the Brunt-Väisälä frequency estimated using the bulk θ gradient ($N = \sqrt{\frac{g(\theta_e - \hat{\theta})}{\hat{\theta}z}}$).
 154 Using the definition for buoyancy length scale ($L_B = \frac{\sigma_w}{N}$) (Mahrt, 1979; Moum, 1996;
 155 Sorbjan, 2006; Sorbjan & Balsley, 2008; Mahrt et al., 2012) we can write

$$156 \quad \Lambda = \frac{L_B}{\sqrt{2}z}. \quad (6)$$

157 Hence in the case of LAI \approx 0, the criterium for the flow to couple with the surface (Eq.
 158 3) can be described with the ratio between L_B and height z .

159 3 Data and instrumentation

160 Measurements were collected at two contrasting locations: observations at Hyytiälä
 161 boreal pine forest (61.845°N, 24.289°E, 181 m a.s.l) and during "Fluxes over snow-covered
 162 surfaces II" (FLOSS-II) campaign above snow-covered rangeland (40.659°N, 106.324°W,
 163 2477 m a.s.l). Hyytiälä is part of the ICOS measurement network (Franz et al., 2018)
 164 and has contributed to the global measurement network FLUXNET since the initiation
 165 of the site in 1996. The forest is governed by Scots pines (*Pinus Sylvestris*) with approx-
 166 imate tree height of 17 m. One-sided LAI of the forest is 4 m² m⁻² and the canopy layer
 167 is between 10 and 17 m. Turbulence profiles within the forest have been studied in Launiainen
 168 et al. (2007). In this study observations made during summer 2019 (25 May to 30 Sep)
 169 were utilised. The measurement configuration consisted of vertical fiber-optic based dis-
 170 tributed temperature sensing (DTS) observations (until 10 July), EC flux measurements
 171 (27 m height) (Rebmann et al., 2018) and temperature and CO₂ concentration profiles
 172 (Montagnani et al., 2018). For details, see Peltola, Lapo, Martinkauppi, et al. (2020),
 173 however there were four notable differences: 1) 10-min averaging period was used, 2) single-
 174 ended data (25 May to 3 June) were also included, 3) both directions in the double-ended

175 configuration were utilised and 4) the DTS temperature observations were denoised using
 176 singular value decomposition prior to analysis (Epps & Krivitzky, 2019). Note that
 177 denoising has an effect only on Fig. 2 since otherwise mean profiles were used. When
 178 calculating $w_{e,crit}$, DTS measurements were utilised when available. All the data anal-
 179 yses were restricted to night time periods (global radiation $< 5 \text{ W m}^{-2}$).

180 The observations made during the FLOSS-II measurement campaign (from Dec 2002
 181 to end of March 2003) have been widely utilised in the analysis of vSBL (e.g. Mahrt &
 182 Vickers, 2005, 2006; Mahrt, 2010; Sun et al., 2020). A 30 m tall tower located in a flat
 183 terrain with grass and partial snow-coverage was instrumented with 3D sonic anemome-
 184 ters at seven levels and slow-response thermometers at eight levels. Quality-controlled
 185 and 5 min averaged data were retrieved from <https://doi.org/10.5065/D6QC01XR> (UCAR/NCAR
 186 - Earth Observing Laboratory, 2017).

187 4 Results and discussion

188 4.1 Examples of contrasting flow regimes

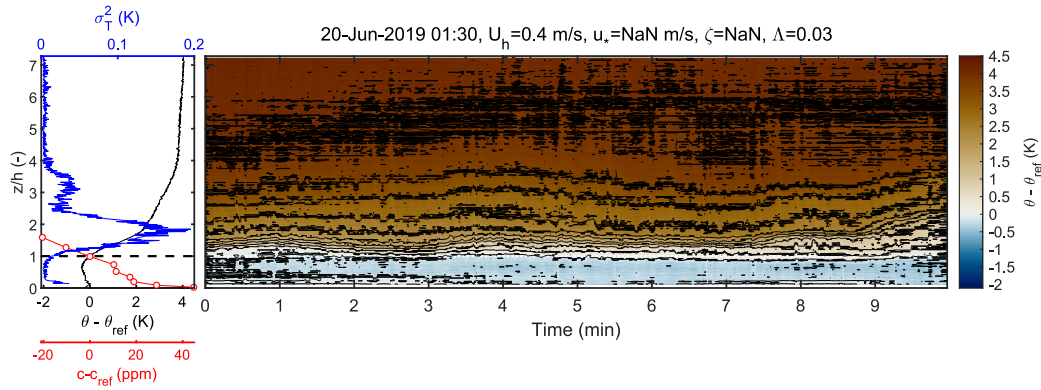
189 Figure 2 shows three 10-min examples of observations in the 125 m tall mast in Hyytiälä
 190 pine forest during contrasting flow regimes: a) quiescent flow which was decoupled from
 191 the ground, b) turbulent flow above canopy which was decoupled from the forest floor
 192 and c) strongly turbulent flow coupled to the ground. Coherent eddies consisting of sweep-
 193 ejection cycle (Thomas & Foken, 2007b; Finnigan et al., 2009) were observed in b) and
 194 c), but not in a). The downward moving sweep phases of the coherent motions can be
 195 identified as the warm tongues penetrating into the cold below-canopy air space, whereas
 196 the ejections bring relatively cold below-canopy air to upper levels above the forest canopy
 197 (due to downward directed heat flux). Note that the sweeping phases in b) did not reach
 198 the forest floor and as a result the flow was decoupled from the ground. This was iden-
 199 tified also with the decoupling metric Λ (see subplot title).

200 CO_2 concentration profiles showed clear differences between the three examples,
 201 as a result from the different mixing regimes. The overall concentration difference be-
 202 tween the highest (27 m) and lowest level (0.5 m) were 67, 26, 9 ppm, respectively. Note
 203 that in case b) this concentration difference resulted almost entirely from the CO_2 pooled
 204 below 8.8 m height, since the CO_2 above this height was effectively flushed out from the
 205 ecosystem by the coherent eddies.

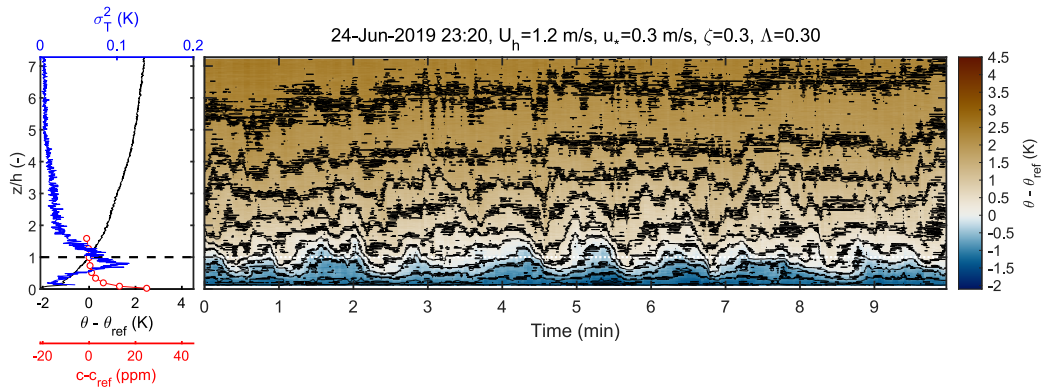
206 4.2 Decoupling in relation to TKE production and transport

207 Above open terrain, Sun et al. (2012) argued that in stably stratified coupled flow
 208 regime turbulent kinetic energy (TKE) should be driven bulk shear (U/z) due to large
 209 eddies and shear production dominating the TKE budget. Hence, they analysed V_{TKE}
 210 ($V_{\text{TKE}} = \sqrt{\text{TKE}} = \sqrt{\sigma_u^2 + 0.5\sigma_v^2 + 0.5\sigma_w^2}$) dependency on U and found a threshold
 211 value for U above which V_{TKE} dependency on U was linear. Observations falling in this
 212 strong wind regime have been considered to relate to coupled flow regime (Mahrt et al.,
 213 2015; Acevedo et al., 2016; Sun et al., 2016; Lan et al., 2018; Freundorfer et al., 2019).
 214 Figures 3a and 3b show V_{TKE} dependency on U for two heights in FLOSS-II dataset,
 215 with data differentiated to separate flow regimes (based on Eq. 3) prior to analysis. In
 216 contrast to Sun et al. (2012), in the coupled regime no U threshold was observed and
 217 V_{TKE} followed the same linear dependence on U regardless of wind speed value. This sug-
 218 gests that in the stable coupled regime TKE was driven by bulk shear as proposed by
 219 Sun et al. (2012), however, this holds regardless of U not confirming the interpretation
 220 in Sun et al. (2012). Similar results were found for the forest site (Hyytiälä) using above-
 221 canopy U and V_{TKE} (not shown). Hence, we argue that flow decoupling cannot be judged
 222 based on U alone.

a) quiescent, decoupled



b) turbulent above-canopy, decoupled



c) turbulent above- and below-canopy, coupled

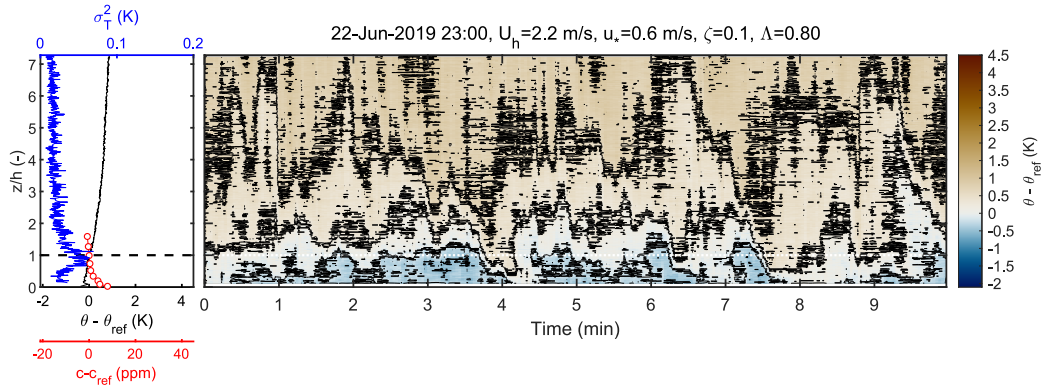


Figure 2. Right: examples of DTS-data during contrasting flow regimes (black lines= θ iso-lines). Left: corresponding temperature variance (blue), mean potential temperature (θ , black) and CO₂ concentration (c , red dots) profiles. c_{ref} and θ_{ref} equal mean c and θ values at canopy height (h).

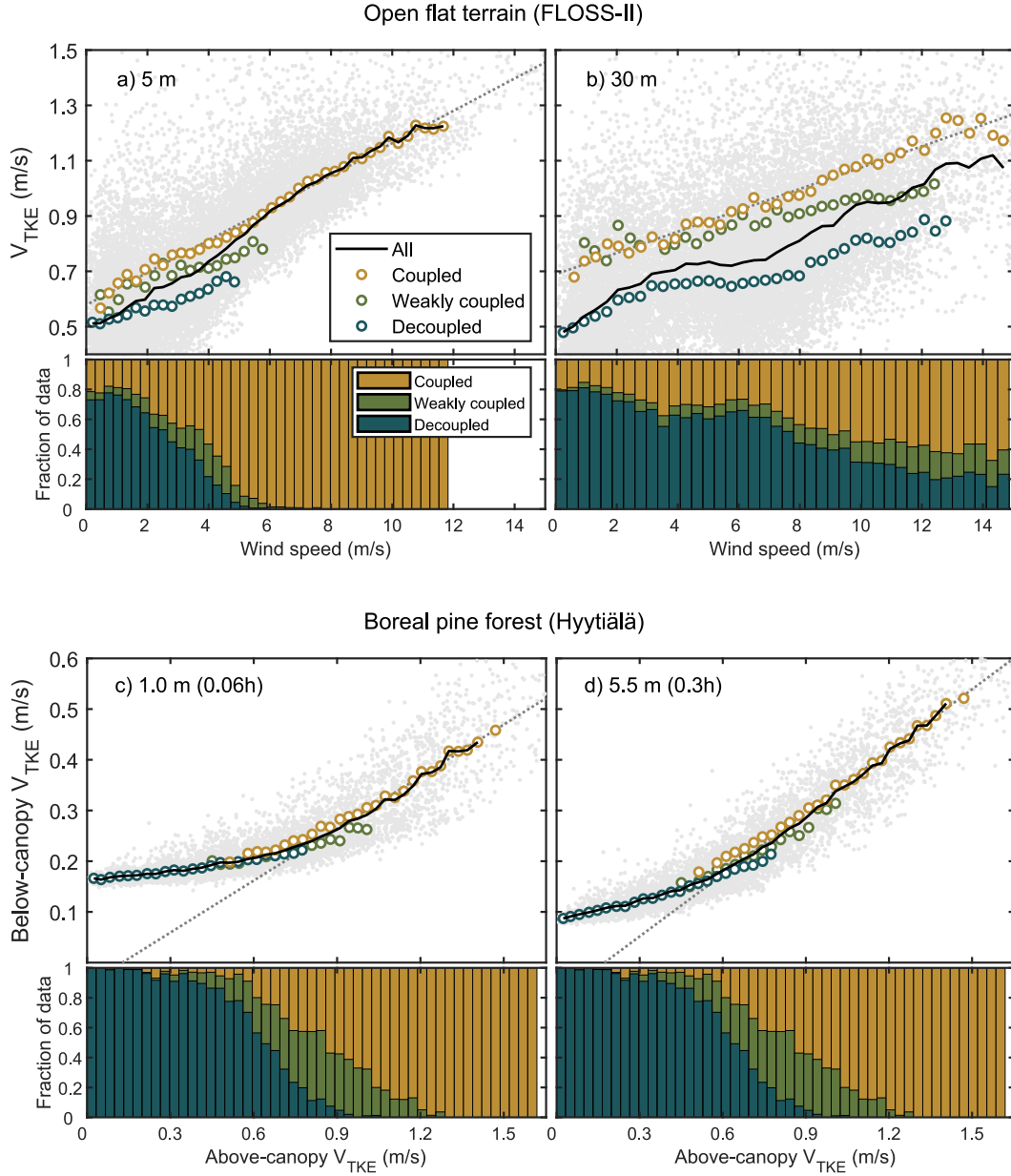


Figure 3. (a and b) V_{TKE} dependency on wind speed (U) at FLOSS-II following Sun et al. (2012). Additionally, data were divided into different coupling regimes (see Eq. 3) prior to analysis. Note that threshold wind speed (Sun et al., 2012) was not observed in the coupled regime. (c and d) comparison of above- and below-canopy V_{TKE} at Hyytiälä following Thomas et al. (2013). Gray dots = all the night-time data, circles and black lines = bin-averages for bins with more than 20 data points. Bottom: fraction of data in the three flow regimes (Eq. 3).

223 In prior studies cross-canopy coupling have been analysed by comparing concur-
 224 rent measurements of σ_w below- and above-canopies (Thomas et al., 2013; Jocher et al.,
 225 2017, 2018; Freundorfer et al., 2019). Linear dependence between the two observations
 226 of σ_w were thought to signal coupling, since downward penetrating canopy-scale sweeps
 227 dominate the below-canopy TKE in coupled flow (Vickers & Thomas, 2013; Russell et
 228 al., 2017; Freundorfer et al., 2019). In accordance with these studies, the coupled flow
 229 regime was typically related to periods with high above-canopy V_{TKE} with a linear de-
 230 pendence between above- and below-canopy V_{TKE} (Figs. 3c and 3d). In contrast, low
 231 above-canopy V_{TKE} was related to decoupled regime. In this regime, below-canopy TKE
 232 was dominated by Kármán vortex streets created behind trees and hence independent
 233 of above-canopy TKE (Cava et al., 2008; Russell et al., 2017) since downward propagat-
 234 ing sweeps did not reach the below-canopy air space (see also Fig. 2b). In our study, the
 235 wake-production generated a clear secondary peak in turbulence spectra (especially in
 236 1 m height data) at the vortex shedding frequency based on constant Strouhal number,
 237 U and tree trunk diameter (not shown). At intermediate above-canopy V_{TKE} levels (0.5...0.8
 238 m/s) the observations related to coupled flow regime departed from the linear depen-
 239 dence observed at higher V_{TKE} values. This might be due to importance of both, wake-
 240 production and sweeps, on below-canopy TKE at these above-canopy TKE levels and
 241 further analyses are warranted.

242 4.3 Turbulent fluxes in the coupled and decoupled layer

243 The sensible heat flux (H) profiles in the FLOSS-II dataset were analysed in the
 244 view of flow decoupling dependency on height (Eq. 6, Sect. 4.4.1). Nocturnal flux pro-
 245 files were calculated so that each of the seven measurement heights was used as the high-
 246 est observational level identified to be coupled with the surface (denoted with z_{co}). Hence
 247 observations below and above z_{co} correspond to coupled and decoupled layers, respec-
 248 tively. The fluxes were normalised with the H values at height z_{co} (H_{co}). Below z_{co} nearly
 249 constant H was observed, whereas above z_{co} the flux H decreased with height, since the
 250 flow above z_{co} was not connected to the surface (Fig. 4a). In the coupled air layer (i.e.
 251 below z_{co}), bin-averaged H was between $0.95H_{co}$ and $1.18H_{co}$ in agreement with the typ-
 252 ical notion for constant-flux layer flows where the vertical turbulent fluxes are expected
 253 to vary by $\pm 10\%$. Note that discrepancies between flux footprints at different heights
 254 and biases stemming from instrument calibrations may have also influenced the observed
 255 H profiles.

256 CO_2 fluxes measured above the Hyytiälä forest during night depended on the de-
 257 gree of coupling (i.e. Λ) when $\Lambda < 0.61$, whereas in the coupled regime the fluxes were
 258 independent of Λ due to direct coupling of flux measurement height with the ground with
 259 turbulent mixing being no longer limiting. Figs. 4a and 4b shows physically the same
 260 phenomenon, but for different sites. Fluxes above z_{co} (Fig. 4a) and during periods with
 261 $\Lambda < 0.61$ (Fig. 4b) correspond to decoupled flow, whereas on the contrary above z_{co}
 262 and during periods with $\Lambda \geq 0.61$ correspond to coupled flow.

263 These results suggest that the method proposed in Sect. 2 can be used to estimate
 264 the depth of the layer that was coupled with the surface and hence e.g. to assess whether
 265 the observed turbulent fluxes related to the exchange of heat (FLOSS-II) or CO_2 (Hyytiälä)
 266 on the surface. Note that these results were obtained at two contrasting measurement
 267 sites without site-specific thresholds. This is due to using a ratio of variables related to
 268 kinetic energy (σ_w) and the energy required to couple with the ground ($w_{e,crit}$) in the
 269 analysis, instead of using σ_w (Acevedo et al., 2009; Thomas et al., 2013; Jocher et al.,
 270 2018) or related variables (u_* , U) (e.g. Gu et al., 2005; Sun et al., 2012) alone. Further-
 271 more, this ratio does not depend on the source for the turbulent mixing in any way, it
 272 merely compares the existing kinetic energy to the energy needed to couple with the ground.
 273 Hence the decoupling metric should be applicable also in situations when the source does

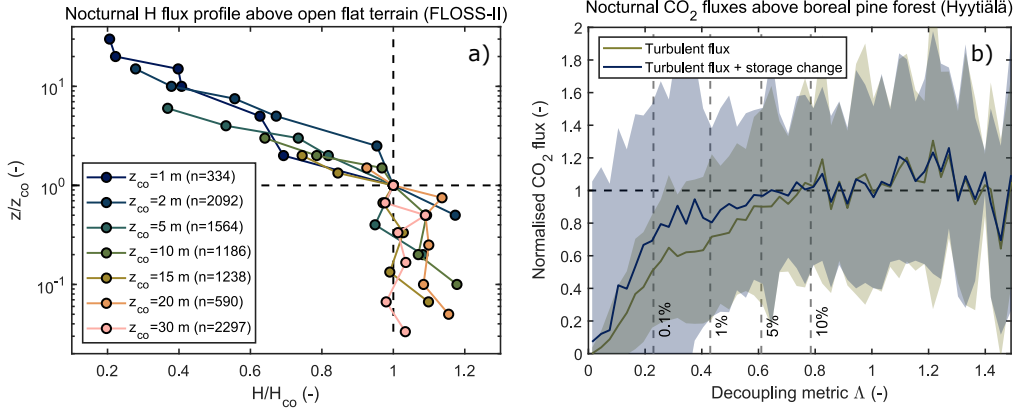


Figure 4. The physical interpretation of the coupling metric for (a) sensible heat profiles at FLOSS-II and (b) cross-canopy coupling of carbon dioxide at Hyytiälä. a): Normalised sensible heat flux (H) profiles (bin medians) observed at FLOSS-II. Profiles were calculated from periods when height z_{co} was coupled with the surface (cf. Eq. 3), but heights above z_{co} were not. Fluxes were normalised with H observed at z_{co} (H_{co}) b): Normalised nocturnal CO_2 fluxes measured at Hyytiälä plotted against Λ (lines=bin means, areas= $\pm\sigma$). Data were filtered based on stationarity criteria (Foken & Wichura, 1996). The storage change term (Finnigan, 2006) was also included. Fluxes were normalised with 2-week running means of nocturnal CO_2 fluxes during coupled regime. Vertical dashed lines = fraction of w' data below $w_{e,crit}$.

274 not conform with the traditional boundary layer (e.g. upside down boundary layer) (Mahrt et al., 2013; Mahrt, 2014).
275

276 4.4 Controls on flow decoupling

277 4.4.1 Flows above short vegetation

278 Above short vegetation (i.e. $LAI \approx 0$), $w_{e,crit}$ depends linearly on z and N (Eq.
279 5) and the definition for coupling (Eq. 3) can be written as

$$280 \sigma_w \geq 0.61\sqrt{2}zN. \quad (7)$$

281 Hence at a given value for N , the σ_w needed to couple the flow with the surface increases
282 linearly with height. This is in line with prior experimental findings (Mahrt et al., 2013;
283 Acevedo et al., 2016). The increase reflects the fact that the kinetic energy of downward
284 moving air parcel needs to be higher when the height increases since there is a thicker
285 air column below the air parcel within which the buoyancy force opposes its movement,
286 i.e. the potential energy of the air parcel increases with height. In the FLOSS-II dataset
287 rarely the upper level was identified to be coupled with the surface when the observa-
288 tion level below was not (less than 1% of observations). In general the lower levels were
289 observed to be coupled with the surface more frequently than the upper levels, for in-
290 stance 5 m height was coupled with the surface 64 % of time, whereas 20 m height only
291 39 % of time.

292 4.4.2 Flows above tall vegetation

293 In the case of neutral stratification below canopy height, using Eq. 4 the definition
294 for coupling (Eq. 3) can be written as

$$295 I_w \geq 1.22\gamma\hat{c}_dLAI, \quad (8)$$

296 where I_w is the vertical turbulence intensity at the canopy height ($I_w = \frac{\sigma_w}{U_h}$). Note the
 297 similarity between the right hand side of Eq. 8 and the ratio between canopy height and
 298 coherent eddy penetration depth in Nepf et al. (2007), Cava et al. (2008) and Ghisalberti
 299 (2009) (i.e. $\propto \hat{c}_d \text{LAI}$) which describes whether the coherent canopy eddies are interact-
 300 ing with the surface or not. At the Hyytiälä site in near neutral conditions above the
 301 forest I_w was on average 0.26, whereas the limit for decoupling calculated using Eq. 8
 302 was 0.20, indicating coupling at this site in near-neutral conditions. In contrast, Thomas
 303 et al. (2013) observed frequent decoupling above their dense forest ($\text{PAI}=9.4 \text{ m}^2\text{m}^{-2}$)
 304 even during daytime despite similar I_w levels (0.25-0.30) and the decoupling could have
 305 been predicted with Eq. 8. It should be noted however that γ and \hat{c}_d depend on canopy
 306 architecture (Amiro, 1990a, 1990b) and the influence of these parameters should be in-
 307 vestigated. Clearly this method should be tested across range of sites with contrasting
 308 canopies, albeit similarities to the studies of Nepf et al. (2007), Cava et al. (2008) and
 309 Ghisalberti (2009) do suggest of a more general applicability.

310 5 Conclusions

311 Poor understanding of the very stable boundary layer is an obstacle for all scien-
 312 tific studies investigating surface-atmosphere interactions, in particular in the case of canopy
 313 flows. Here, we propose a novel simple first-principle based scheme to identify periods
 314 when the air flow is not in interaction with the underlying surface (i.e. it is decoupled).
 315 It was shown to correctly identify periods when the measured turbulent fluxes were not
 316 representative of the fluxes at the surface. The metric for flow decoupling based on this
 317 concept enabled analytical derivation of flow decoupling dependency on height, strat-
 318 ification and leaf area index. The approach is an improvement to the commonly used
 319 methods based on e.g. friction velocity filtering since 1) the proposed approach takes into
 320 account also changes in forces hindering the coupling (canopy drag, stable stratification)
 321 unlike traditional methods which utilise metrics for turbulent mixing or production alone
 322 and 2) it is based on first principles and not on ad-hoc empirical correlations. From a
 323 practical point-of-view, the approach requires only basic micrometeorological measure-
 324 ments (turbulence measurements at one height and temperature profile below it) in ad-
 325 dition to knowledge of canopy density and hence should be applicable at most flux sites
 326 through the complete gradient from locations with short canopies to dense tall forests.

327 Acknowledgments

328 FLOSS-II data were provided by NCAR/EOL under the sponsorship of the National Sci-
 329 ence Foundation (<https://data.eol.ucar.edu/>). University of Helsinki, in particular Timo
 330 Vesala and technical staff at the Hyytiälä research station, are acknowledged for enabling
 331 the measurement campaign in Hyytiälä. OP is supported by the postdoctoral researcher
 332 project (decision 315424) funded by the Academy of Finland. KL and CT received fund-
 333 ing from the European Research Council (ERC) under the European Union's Horizon
 334 2020 research and innovation program (grant agreement No 724629, project DarkMix).
 335 FLOSS-II data can be acquired at <https://doi.org/10.5065/D6QC01XR> and Hyytiälä
 336 data were uploaded to Zenodo (Peltola, Lapo, & Thomas, 2020) and will be published
 337 upon acceptance of this manuscript.

338 References

- 339 Acevedo, O. C., Mahrt, L., Puhales, F. S., Costa, F. D., Medeiros, L. E., &
 340 Degrazia, G. A. (2016, 1). Contrasting structures between the decou-
 341 pled and coupled states of the stable boundary layer. *Quarterly Journal*
 342 *of the Royal Meteorological Society*, 142(695), 693–702. Retrieved from
 343 <https://doi.org/10.1002/qj.2693> doi: 10.1002/qj.2693
 344 Acevedo, O. C., Moraes, O. L. L., Degrazia, G. A., Fitzjarrald, D. R., Manzi, A. O.,

- 345 & Campos, J. G. (2009). Is friction velocity the most appropriate scale for
 346 correcting nocturnal carbon dioxide fluxes? *Agricultural and Forest Mete-*
 347 *orology*, *149*(1), 1–10. Retrieved from [http://www.sciencedirect.com/](http://www.sciencedirect.com/science/article/pii/S0168192308001962)
 348 [science/article/pii/S0168192308001962](http://www.sciencedirect.com/science/article/pii/S0168192308001962) doi: [https://doi.org/10.1016/](https://doi.org/10.1016/j.agrformet.2008.06.014)
 349 [j.agrformet.2008.06.014](https://doi.org/10.1016/j.agrformet.2008.06.014)
- 350 Amiro, B. D. (1990a). Comparison of turbulence statistics within three boreal for-
 351 est canopies. *Boundary-Layer Meteorology*, *51*(1), 99–121. Retrieved from
 352 <https://doi.org/10.1007/BF00120463> doi: 10.1007/BF00120463
- 353 Amiro, B. D. (1990b). Drag coefficients and turbulence spectra within three boreal
 354 forest canopies. *Boundary-Layer Meteorology*, *52*(3), 227–246. Retrieved from
 355 <https://doi.org/10.1007/BF00122088> doi: 10.1007/BF00122088
- 356 Aubinet, M., Feigenwinter, C., Heinesch, B., Bernhofer, C., Canepa, E., Lindroth,
 357 A., ... Van Gorsel, E. (2010). Direct advection measurements do not
 358 help to solve the night-time CO₂ closure problem: Evidence from three dif-
 359 ferent forests. *Agricultural and Forest Meteorology*, *150*(5), 655–664. doi:
 360 [10.1016/j.agrformet.2010.01.016](https://doi.org/10.1016/j.agrformet.2010.01.016)
- 361 Baldocchi, D. (2014, 6). Measuring fluxes of trace gases and energy between
 362 ecosystems and the atmosphere – the state and future of the eddy covari-
 363 ance method. *Global Change Biology*, *20*(12), 3600–3609. Retrieved from
 364 <https://doi.org/10.1111/gcb.12649> doi: 10.1111/gcb.12649
- 365 Cava, D., Katul, G. G., Semperviva, A. M., Giostra, U., & Scrimieri, A. (2008). On
 366 the Anomalous Behaviour of Scalar Flux–Variance Similarity Functions Within
 367 the Canopy Sub-layer of a Dense Alpine Forest. *Boundary-Layer Meteorology*,
 368 *128*(1), 33. Retrieved from <https://doi.org/10.1007/s10546-008-9276-z>
 369 doi: 10.1007/s10546-008-9276-z
- 370 Cescatti, A., & Marcolla, B. (2004). Drag coefficient and turbulence intensity
 371 in conifer canopies. *Agricultural and Forest Meteorology*, *121*(3), 197–206.
 372 Retrieved from [http://www.sciencedirect.com/science/article/pii/](http://www.sciencedirect.com/science/article/pii/S0168192303002028)
 373 [S0168192303002028](http://www.sciencedirect.com/science/article/pii/S0168192303002028) doi: <https://doi.org/10.1016/j.agrformet.2003.08.028>
- 374 Epps, B. P., & Krivitzky, E. M. (2019). Singular value decomposition of noisy data:
 375 noise filtering. *Experiments in Fluids*, *60*(8), 126. Retrieved from [https://doi](https://doi.org/10.1007/s00348-019-2768-4)
 376 [.org/10.1007/s00348-019-2768-4](https://doi.org/10.1007/s00348-019-2768-4) doi: 10.1007/s00348-019-2768-4
- 377 Finnigan, J. (2000, 1). Turbulence in Plant Canopies. *Annual Review of Fluid Me-*
 378 *chanics*, *32*(1), 519–571. Retrieved from [https://doi.org/10.1146/annurev](https://doi.org/10.1146/annurev.fluid.32.1.519)
 379 [.fluid.32.1.519](https://doi.org/10.1146/annurev.fluid.32.1.519) doi: 10.1146/annurev.fluid.32.1.519
- 380 Finnigan, J. (2006). The storage term in eddy flux calculations. *Agricultural and*
 381 *Forest Meteorology*, *136*(3-4), 108–113. doi: 10.1016/j.agrformet.2004.12.010
- 382 Finnigan, J., Shaw, R. H., & Patton, E. G. (2009). Turbulence structure above
 383 a vegetation canopy. *Journal of Fluid Mechanics*, *637*, 387–424. Retrieved
 384 from [https://www.cambridge.org/core/article/turbulence-structure](https://www.cambridge.org/core/article/turbulence-structure-above-a-vegetation-canopy/575D5DD5B6CFD8837D3C765E04216E41)
 385 [-above-a-vegetation-canopy/575D5DD5B6CFD8837D3C765E04216E41](https://www.cambridge.org/core/article/turbulence-structure-above-a-vegetation-canopy/575D5DD5B6CFD8837D3C765E04216E41) doi:
 386 DOI:10.1017/S0022112009990589
- 387 Foken, T., & Wichura, B. (1996). Tools for quality assessment of surface-based flux
 388 measurements. *Agricultural and Forest Meteorology*, *78*(1-2), 83–105.
- 389 Franz, D., Acosta, M., Altimir, N., Arriga, N., Arrouays, D., Aubinet, M., ...
 390 Vesala, T. (2018). Towards long-Term standardised carbon and greenhouse
 391 gas observations for monitoring Europe’s terrestrial ecosystems: A review.
 392 *International Agrophysics*, *32*(4). doi: 10.1515/intag-2017-0039
- 393 Freundorfer, A., Rehberg, I., Law, B. E., & Thomas, C. (2019). Forest wind regimes
 394 and their implications on cross-canopy coupling. *Agricultural and Forest Me-*
 395 *teorology*, *279*, 107696. Retrieved from [http://www.sciencedirect.com/](http://www.sciencedirect.com/science/article/pii/S0168192319303120)
 396 [science/article/pii/S0168192319303120](http://www.sciencedirect.com/science/article/pii/S0168192319303120) doi: [https://doi.org/10.1016/](https://doi.org/10.1016/j.agrformet.2019.107696)
 397 [j.agrformet.2019.107696](https://doi.org/10.1016/j.agrformet.2019.107696)
- 398 Friedlingstein, P., Jones, M. W., O’Sullivan, M., Andrew, R. M., Hauck, J., Peters,
 399 G. P., ... Zaehle, S. (2019, 12). Global Carbon Budget 2019. *Earth Syst.*

- 400 *Sci. Data*, 11(4), 1783–1838. Retrieved from [https://essd.copernicus.org/](https://essd.copernicus.org/articles/11/1783/2019/https://essd.copernicus.org/articles/11/1783/2019/essd-11-1783-2019.pdf)
 401 [articles/11/1783/2019/https://essd.copernicus.org/articles/11/](https://essd.copernicus.org/articles/11/1783/2019/https://essd.copernicus.org/articles/11/1783/2019/essd-11-1783-2019.pdf)
 402 [1783/2019/essd-11-1783-2019.pdf](https://essd.copernicus.org/articles/11/1783/2019/https://essd.copernicus.org/articles/11/1783/2019/essd-11-1783-2019.pdf) doi: 10.5194/essd-11-1783-2019
- 403 Ghisalberti, M. (2009). Obstructed shear flows: similarities across systems and
 404 scales. *Journal of Fluid Mechanics*, 641, 51–61. Retrieved from [https://](https://www.cambridge.org/core/article/obstructed-shear-flows-similarities-across-systems-and-scales/57CB658F47B27DB2A24B03236B3AD25B)
 405 [www.cambridge.org/core/article/obstructed-shear-flows-similarities](https://www.cambridge.org/core/article/obstructed-shear-flows-similarities-across-systems-and-scales/57CB658F47B27DB2A24B03236B3AD25B)
 406 [-across-systems-and-scales/57CB658F47B27DB2A24B03236B3AD25B](https://www.cambridge.org/core/article/obstructed-shear-flows-similarities-across-systems-and-scales/57CB658F47B27DB2A24B03236B3AD25B) doi:
 407 DOI:10.1017/S0022112009992175
- 408 Grachev, A. A., Andreas, E. L., Fairall, C. W., Guest, P. S., & Persson, P. O. G.
 409 (2013). The Critical Richardson Number and Limits of Applicability of
 410 Local Similarity Theory in the Stable Boundary Layer. *Boundary-Layer*
 411 *Meteorology*, 147(1), 51–82. Retrieved from [https://doi.org/10.1007/](https://doi.org/10.1007/s10546-012-9771-0)
 412 [s10546-012-9771-0](https://doi.org/10.1007/s10546-012-9771-0) doi: 10.1007/s10546-012-9771-0
- 413 Gu, L., Falge, E. M., Boden, T., Baldocchi, D. D., Black, T. A., Saleska, S. R., ...
 414 Xu, L. (2005). Objective threshold determination for nighttime eddy flux
 415 filtering. *Agricultural and Forest Meteorology*, 128(3), 179–197. Retrieved from
 416 <http://www.sciencedirect.com/science/article/pii/S0168192304003053>
 417 doi: <https://doi.org/10.1016/j.agrformet.2004.11.006>
- 418 Inoue, E. (1963). On the Turbulent Structure of Airflow within Crop Canopies.
 419 *Journal of the Meteorological Society of Japan. Ser. II*, 41(6), 317–326. doi: 10
 420 .2151/jmsj1923.41.6{_}317
- 421 Jocher, G., Marshall, J., Nilsson, M. B., Linder, S., De Simon, G., Hörnlund, T., ...
 422 Peichl, M. (2018, 2). Impact of Canopy Decoupling and Subcanopy Advection
 423 on the Annual Carbon Balance of a Boreal Scots Pine Forest as Derived From
 424 Eddy Covariance. *Journal of Geophysical Research: Biogeosciences*, 123(2),
 425 303–325. Retrieved from <https://doi.org/10.1002/2017JG003988> doi:
 426 10.1002/2017JG003988
- 427 Jocher, G., Ottosson Löfvenius, M., De Simon, G., Hörnlund, T., Linder, S., Lund-
 428 mark, T., ... Peichl, M. (2017). Apparent winter CO₂ uptake by a boreal
 429 forest due to decoupling. *Agricultural and Forest Meteorology*, 232, 23–34.
 430 Retrieved from [http://www.sciencedirect.com/science/article/pii/](http://www.sciencedirect.com/science/article/pii/S0168192316303495)
 431 [S0168192316303495](http://www.sciencedirect.com/science/article/pii/S0168192316303495) doi: <https://doi.org/10.1016/j.agrformet.2016.08.002>
- 432 Kruijt, B., Malhi, Y., Lloyd, J., Norbre, A. D., Miranda, A. C., Pereira, M. G. P.,
 433 ... Grace, J. (2000). Turbulence Statistics Above And Within Two Ama-
 434 zon Rain Forest Canopies. *Boundary-Layer Meteorology*, 94(2), 297–
 435 331. Retrieved from <https://doi.org/10.1023/A:1002401829007> doi:
 436 10.1023/A:1002401829007
- 437 Lan, C., Liu, H., Li, D., Katul, G. G., & Finn, D. (2018, 8). Distinct Turbulence
 438 Structures in Stably Stratified Boundary Layers With Weak and Strong
 439 Surface Shear. *Journal of Geophysical Research: Atmospheres*, 123(15),
 440 7839–7854. Retrieved from <https://doi.org/10.1029/2018JD028628> doi:
 441 10.1029/2018JD028628
- 442 Launiainen, S., Vesala, T., Mölder, M., Mammarella, I., Smolander, S., Rannik, , ...
 443 Katul, G. (2007, 1). Vertical variability and effect of stability on turbulence
 444 characteristics down to the floor of a pine forest. *Tellus B: Chemical and Phys-*
 445 *ical Meteorology*, 59(5), 919–936. Retrieved from [https://doi.org/10.1111/](https://doi.org/10.1111/j.1600-0889.2007.00313.x)
 446 [j.1600-0889.2007.00313.x](https://doi.org/10.1111/j.1600-0889.2007.00313.x) doi: 10.1111/j.1600-0889.2007.00313.x
- 447 Li, D., Salesky, S. T., & Banerjee, T. (2016). Connections between the Ozmidov
 448 scale and mean velocity profile in stably stratified atmospheric surface layers.
 449 *Journal of Fluid Mechanics*, 797, R3. Retrieved from [https://www.cambridge](https://www.cambridge.org/core/article/connections-between-the-ozmidov-scale-and-mean-velocity-profile-in-stably-stratified-atmospheric-surface-layers/8FCD6918C8A541A494D29B70D839145F)
 450 [.org/core/article/connections-between-the-ozmidov-scale-and-mean](https://www.cambridge.org/core/article/connections-between-the-ozmidov-scale-and-mean-velocity-profile-in-stably-stratified-atmospheric-surface-layers/8FCD6918C8A541A494D29B70D839145F)
 451 [-velocity-profile-in-stably-stratified-atmospheric-surface-layers/](https://www.cambridge.org/core/article/connections-between-the-ozmidov-scale-and-mean-velocity-profile-in-stably-stratified-atmospheric-surface-layers/8FCD6918C8A541A494D29B70D839145F)
 452 [8FCD6918C8A541A494D29B70D839145F](https://www.cambridge.org/core/article/connections-between-the-ozmidov-scale-and-mean-velocity-profile-in-stably-stratified-atmospheric-surface-layers/8FCD6918C8A541A494D29B70D839145F) doi: DOI:10.1017/jfm.2016.311
- 453 Mahrt, L. (1979, 4). Penetrative convection at the top of a growing boundary
 454 layer. *Quarterly Journal of the Royal Meteorological Society*, 105(444), 469–

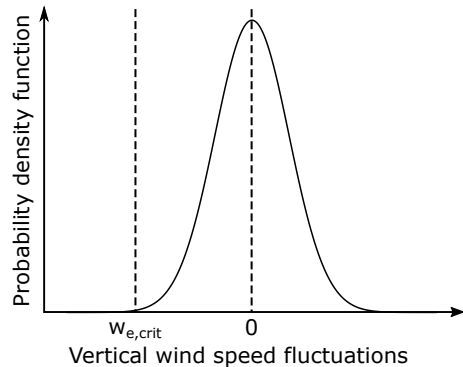
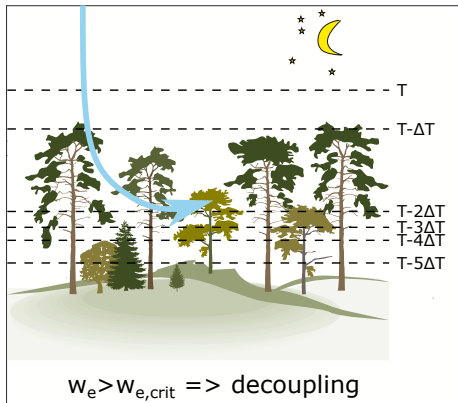
- 455 485. Retrieved from <https://doi.org/10.1002/qj.49710544411> doi:
456 10.1002/qj.49710544411
- 457 Mahrt, L. (2010). Variability and Maintenance of Turbulence in the Very Sta-
458 ble Boundary Layer. *Boundary-Layer Meteorology*, 135(1), 1–18. Re-
459 trieved from <https://doi.org/10.1007/s10546-009-9463-6> doi:
460 10.1007/s10546-009-9463-6
- 461 Mahrt, L. (2014). Stably Stratified Atmospheric Boundary Layers. *An-
462 nual Review of Fluid Mechanics*, 46(1), 23–45. Retrieved from [http://
463 www.annualreviews.org/doi/abs/10.1146/annurev-fluid-010313-141354](http://www.annualreviews.org/doi/abs/10.1146/annurev-fluid-010313-141354)
464 doi: 10.1146/annurev-fluid-010313-141354
- 465 Mahrt, L., Richardson, S., Seaman, N., & Stauffer, D. (2012). Turbulence in the
466 nocturnal boundary layer with light and variable winds. *Quarterly Journal
467 of the Royal Meteorological Society*, 138(667), 1430–1439. Retrieved from
468 <http://dx.doi.org/10.1002/qj.1884> doi: 10.1002/qj.1884
- 469 Mahrt, L., Sun, J., Blumen, W., Delany, T., & Oncley, S. (1998). Nocturnal
470 boundary-layer regimes. *Boundary-Layer Meteorology*, 88(2), 255–278.
- 471 Mahrt, L., Sun, J., & Stauffer, D. (2015). Dependence of Turbulent Velocities on
472 Wind Speed and Stratification. *Boundary-Layer Meteorology*, 155(1), 55–
473 71. Retrieved from <https://doi.org/10.1007/s10546-014-9992-5> doi:
474 10.1007/s10546-014-9992-5
- 475 Mahrt, L., Thomas, C., Richardson, S., Seaman, N., Stauffer, D., & Zeeman, M.
476 (2013). Non-stationary Generation of Weak Turbulence for Very Stable
477 and Weak-Wind Conditions. *Boundary-Layer Meteorology*, 147(2), 179–
478 199. Retrieved from <https://doi.org/10.1007/s10546-012-9782-x> doi:
479 10.1007/s10546-012-9782-x
- 480 Mahrt, L., Thomas, C. K., Grachev, A. A., & Persson, P. O. G. (2018). Near-
481 Surface Vertical Flux Divergence in the Stable Boundary Layer. *Boundary-
482 Layer Meteorology*, 169(3), 373–393. Retrieved from [https://doi.org/
483 10.1007/s10546-018-0379-x](https://doi.org/10.1007/s10546-018-0379-x) doi: 10.1007/s10546-018-0379-x
- 484 Mahrt, L., & Vickers, D. (2005). Boundary-Layer Adjustment Over Small-Scale
485 Changes of Surface Heat Flux. *Boundary-Layer Meteorology*, 116(2), 313–
486 330. Retrieved from <https://doi.org/10.1007/s10546-004-1669-z> doi:
487 10.1007/s10546-004-1669-z
- 488 Mahrt, L., & Vickers, D. (2006). Extremely Weak Mixing in Stable Conditions.
489 *Boundary-Layer Meteorology*, 119(1), 19–39. Retrieved from [https://
490 doi.org/10.1007/s10546-005-9017-5](https://doi.org/10.1007/s10546-005-9017-5) doi: 10.1007/s10546-005-9017-5
- 491 Montagnani, L., Grünwald, T., Kowalski, A., Mammarella, I., Merbold, L., Metzger,
492 S., ... Siebicke, L. (2018). Estimating the storage term in eddy covariance
493 measurements: the ICOS methodology. *International Agrophysics*, 32(4), 551–
494 567. Retrieved from <http://dx.doi.org/10.1515/intag-2017-0037> doi:
495 10.1515/intag-2017-0037
- 496 Moum, J. N. (1996, 6). Energy-containing scales of turbulence in the ocean
497 thermocline. *Journal of Geophysical Research: Oceans*, 101(C6), 14095–
498 14109. Retrieved from <https://doi.org/10.1029/96JC00507> doi:
499 10.1029/96JC00507
- 500 Nepf, H., Ghisalberti, M., White, B., & Murphy, E. (2007, 4). Retention time and
501 dispersion associated with submerged aquatic canopies. *Water Resources Re-
502 search*, 43(4). Retrieved from <https://doi.org/10.1029/2006WR005362> doi:
503 10.1029/2006WR005362
- 504 Nieuwstadt, F. T. M. (1984, 7). The Turbulent Structure of the Stable, Nocturnal
505 Boundary Layer. *Journal of the Atmospheric Sciences*, 41(14), 2202–2216.
506 Retrieved from [https://doi.org/10.1175/1520-0469\(1984\)041%3C2202:
507 TTSOTS%3E2.0.CO;2](https://doi.org/10.1175/1520-0469(1984)041%3C2202:TTSOTS%3E2.0.CO;2) <http://0.0.0.2> doi: 10.1175/1520-0469(1984)041<2202:
508 TTSOTS>2.0.CO;2
- 509 Peltola, O., Lapo, K., Martinkauppi, I., O'Connor, E., Thomas, C. K., & Vesala,

- 510 T. (2020). Suitability of fiber-optic distributed temperature sensing to
 511 reveal mixing processes and higher-order moments at the forest-air inter-
 512 face. *Atmospheric Measurement Techniques Discussions*, 2020, 1–31. Re-
 513 trieved from <https://amt.copernicus.org/preprints/amt-2020-260/> doi:
 514 10.5194/amt-2020-260
- 515 Peltola, O., Lapo, K., & Thomas, C. (2020). *Dataset for "A physics-based universal*
 516 *indicator for vertical decoupling and mixing across canopies architectures and*
 517 *dynamic stabilities"*. doi: 10.5281/zenodo.4250443
- 518 Poggi, D., Katul, G. G., & Albertson, J. D. (2004). Momentum Transfer and Turbu-
 519 lent Kinetic Energy Budgets within a Dense Model Canopy. *Boundary-Layer*
 520 *Meteorology*, 111(3), 589–614. Retrieved from [https://doi.org/10.1023/B:](https://doi.org/10.1023/B:BOUN.0000016502.52590.af)
 521 [BOUN.0000016502.52590.af](https://doi.org/10.1023/B:BOUN.0000016502.52590.af) doi: 10.1023/B:BOUN.0000016502.52590.af
- 522 Poggi, D., Porporato, A., Ridolfi, L., Albertson, J. D., & Katul, G. G. (2004). The
 523 Effect of Vegetation Density on Canopy Sub-Layer Turbulence. *Boundary-*
 524 *Layer Meteorology*, 111(3), 565–587. Retrieved from [https://doi.org/](https://doi.org/10.1023/B:BOUN.0000016576.05621.73)
 525 [10.1023/B:BOUN.0000016576.05621.73](https://doi.org/10.1023/B:BOUN.0000016576.05621.73) doi: 10.1023/B:BOUN.0000016576
 526 .05621.73
- 527 Raupach, M. R., Finnigan, J. J., & Brunei, Y. (1996). Coherent eddies and tur-
 528 bulence in vegetation canopies: The mixing-layer analogy. *Boundary-Layer*
 529 *Meteorology*, 78(3), 351–382. Retrieved from [https://doi.org/10.1007/](https://doi.org/10.1007/BF00120941)
 530 [BF00120941](https://doi.org/10.1007/BF00120941) doi: 10.1007/BF00120941
- 531 Rebmann, C., Aubinet, M., Schmid, H., Arriga, N., Aurela, M., Burba, G., ...
 532 Franz, D. (2018). ICOS eddy covariance flux-station site setup: a review. *In-*
 533 *ternational Agrophysics*, 32(4), 471–494. Retrieved from [http://dx.doi.org/](http://dx.doi.org/10.1515/intag-2017-0044)
 534 [10.1515/intag-2017-0044](http://dx.doi.org/10.1515/intag-2017-0044) doi: 10.1515/intag-2017-0044
- 535 Russell, E. S., Liu, H., & Lamb, B. (2017, 8). Wavelet spectra within a for-
 536 est subcanopy under different wind directions and stabilities. *Journal of*
 537 *Geophysical Research: Atmospheres*, 122(16), 8399–8409. Retrieved from
 538 <https://doi.org/10.1002/2017JD026817> doi: 10.1002/2017JD026817
- 539 Santana, R. A., Dias-Júnior, C. Q., da Silva, J. T., Fuentes, J. D., do Vale,
 540 R. S., Alves, E. G., ... Manzi, A. O. (2018). Air turbulence charac-
 541 teristics at multiple sites in and above the Amazon rainforest canopy.
 542 *Agricultural and Forest Meteorology*, 260-261, 41–54. Retrieved from
 543 <http://www.sciencedirect.com/science/article/pii/S0168192318301850>
 544 doi: <https://doi.org/10.1016/j.agrformet.2018.05.027>
- 545 Sorbjan, Z. (2006, 5). Local Structure of Turbulence in Stably Stratified Bound-
 546 ary Layers. *Journal of the Atmospheric Sciences*, 63(5), 1526–1537. Retrieved
 547 from <https://doi.org/10.1175/JAS3704.1> doi: 10.1175/JAS3704.1
- 548 Sorbjan, Z., & Balsley, B. B. (2008). Microstructure of Turbulence in the Stably
 549 Stratified Boundary Layer. *Boundary-Layer Meteorology*, 129(2), 191–210. Re-
 550 trieved from <https://doi.org/10.1007/s10546-008-9310-1> doi: 10.1007/
 551 s10546-008-9310-1
- 552 Sun, J., Lenschow, D. H., LeMone, M. A., & Mahrt, L. (2016). The Role of
 553 Large-Coherent-Eddy Transport in the Atmospheric Surface Layer Based
 554 on CASES-99 Observations. *Boundary-Layer Meteorology*, 160(1), 83–
 555 111. Retrieved from <https://doi.org/10.1007/s10546-016-0134-0> doi:
 556 10.1007/s10546-016-0134-0
- 557 Sun, J., Mahrt, L., Banta, R. M., & Pichugina, Y. L. (2012, 1). Turbulence Regimes
 558 and Turbulence Intermittency in the Stable Boundary Layer during CASES-
 559 99. *Journal of the Atmospheric Sciences*, 69(1), 338–351. Retrieved from
 560 <https://doi.org/10.1175/JAS-D-11-082.1> doi: 10.1175/JAS-D-11-082.1
- 561 Sun, J., Takle, E. S., & Acevedo, O. C. (2020). Understanding Physical Processes
 562 Represented by the Monin–Obukhov Bulk Formula for Momentum Transfer.
 563 *Boundary-Layer Meteorology*. Retrieved from [https://doi.org/10.1007/](https://doi.org/10.1007/s10546-020-00546-5)
 564 [s10546-020-00546-5](https://doi.org/10.1007/s10546-020-00546-5) doi: 10.1007/s10546-020-00546-5

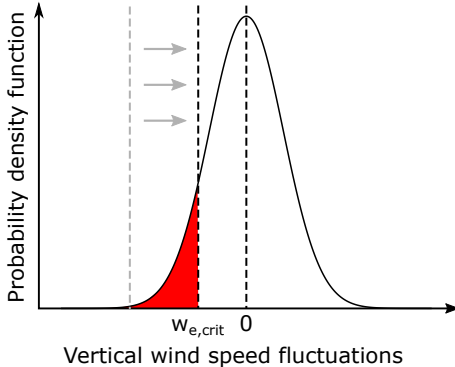
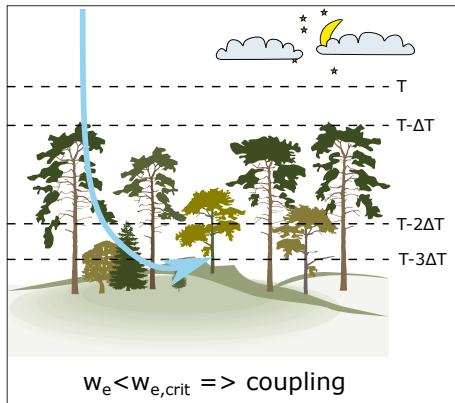
- 565 Thomas, C., & Foken, T. (2007a). Flux contribution of coherent structures and its
566 implications for the exchange of energy and matter in a tall spruce canopy.
567 *Boundary-Layer Meteorology*, *123*(2), 317–337. Retrieved from [https://](https://doi.org/10.1007/s10546-006-9144-7)
568 doi.org/10.1007/s10546-006-9144-7 doi: 10.1007/s10546-006-9144-7
- 569 Thomas, C., & Foken, T. (2007b). Organised Motion in a Tall Spruce Canopy: Tem-
570 poral Scales, Structure Spacing and Terrain Effects. *Boundary-Layer Meteorol-*
571 *ogy*, *122*(1), 123–147. Retrieved from [https://doi.org/10.1007/s10546-006-](https://doi.org/10.1007/s10546-006-9087-z)
572 [9087-z](https://doi.org/10.1007/s10546-006-9087-z) doi: 10.1007/s10546-006-9087-z
- 573 Thomas, C., Martin, J. G., Law, B. E., & Davis, K. (2013). Toward biologically
574 meaningful net carbon exchange estimates for tall, dense canopies: Multi-
575 level eddy covariance observations and canopy coupling regimes in a mature
576 Douglas-fir forest in Oregon. *Agricultural and Forest Meteorology*, *173*, 14–27.
577 Retrieved from [http://www.sciencedirect.com/science/article/pii/](http://www.sciencedirect.com/science/article/pii/S0168192313000051)
578 [S0168192313000051](http://www.sciencedirect.com/science/article/pii/S0168192313000051) doi: <https://doi.org/10.1016/j.agrformet.2013.01.001>
- 579 UCAR/NCAR - Earth Observing Laboratory. (2017). *NCAR/EOL 5 minute Quality*
580 *Controlled ISFF data. Version 1.0. UCAR/NCAR - Earth Observing Labora-*
581 *tory*. doi: <https://doi.org/10.5065/D6QC01XR>
- 582 Vickers, D., & Thomas, C. K. (2013). Some aspects of the turbulence kinetic
583 energy and fluxes above and beneath a tall open pine forest canopy. *Agri-*
584 *cultural and Forest Meteorology*, *181*, 143–151. Retrieved from [http://](http://www.sciencedirect.com/science/article/pii/S0168192313001949)
585 www.sciencedirect.com/science/article/pii/S0168192313001949 doi:
586 <https://doi.org/10.1016/j.agrformet.2013.07.014>
- 587 Watanabe, T. (2004). Large-Eddy Simulation of Coherent Turbulence Structures
588 Associated with Scalar Ramps Over Plant Canopies. *Boundary-Layer Meteo-*
589 *rology*, *112*(2), 307–341. Retrieved from [https://doi.org/10.1023/B:BOUN](https://doi.org/10.1023/B:BOUN.0000027912.84492.54)
590 [.0000027912.84492.54](https://doi.org/10.1023/B:BOUN.0000027912.84492.54) doi: 10.1023/B:BOUN.0000027912.84492.54
- 591 Williams, A. G., Chambers, S., & Griffiths, A. (2013). Bulk Mixing and De-
592 coupling of the Nocturnal Stable Boundary Layer Characterized Using a
593 Ubiquitous Natural Tracer. *Boundary-Layer Meteorology*, *149*(3), 381–
594 402. Retrieved from <https://doi.org/10.1007/s10546-013-9849-3> doi:
595 [10.1007/s10546-013-9849-3](https://doi.org/10.1007/s10546-013-9849-3)
- 596 Yi, C. (2008, 1). Momentum Transfer within Canopies. *Journal of Applied Mete-*
597 *orology and Climatology*, *47*(1), 262–275. Retrieved from [https://doi.org/10](https://doi.org/10.1175/2007JAMC1667.1)
598 [.1175/2007JAMC1667.1](https://doi.org/10.1175/2007JAMC1667.1) doi: 10.1175/2007JAMC1667.1
- 599 Zeeman, M. J., Eugster, W., & Thomas, C. K. (2013). Concurrency of Coher-
600 ent Structures and Conditionally Sampled Daytime Sub-canopy Respiration.
601 *Boundary-Layer Meteorology*, *146*(1), 1–15. Retrieved from [https://doi.org/](https://doi.org/10.1007/s10546-012-9745-2)
602 [10.1007/s10546-012-9745-2](https://doi.org/10.1007/s10546-012-9745-2) doi: 10.1007/s10546-012-9745-2

Figure 1.

a) decoupling



b) coupling despite weak inversion



c) coupling due to strong above canopy turbulence

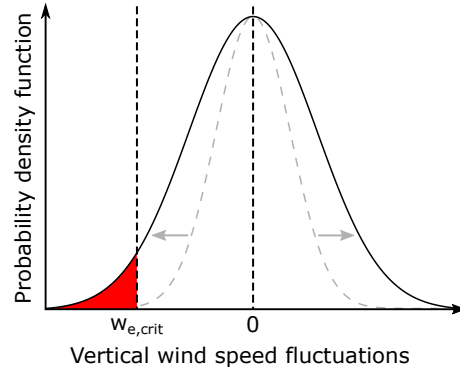
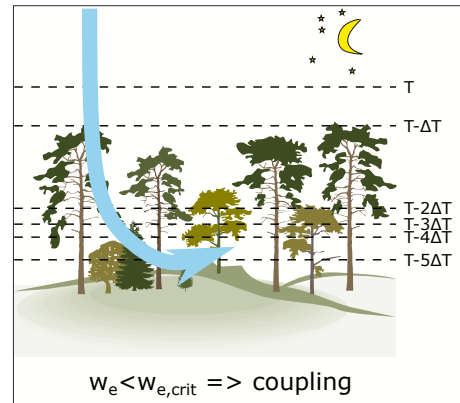
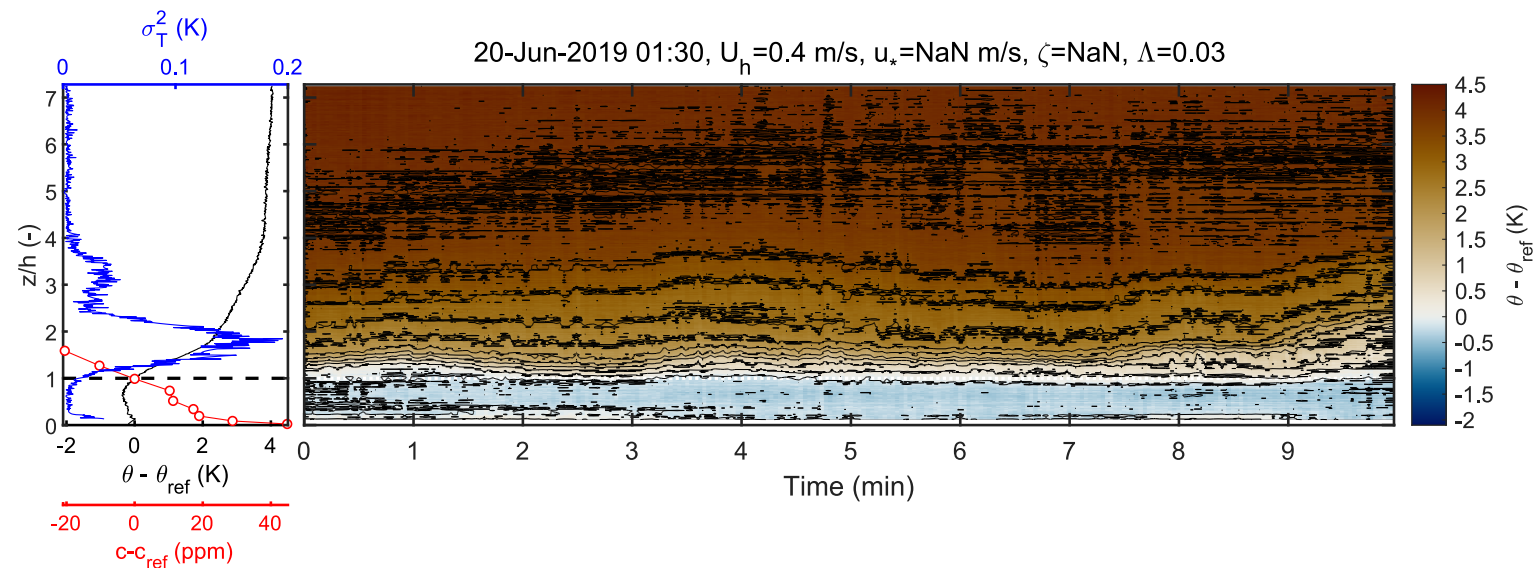
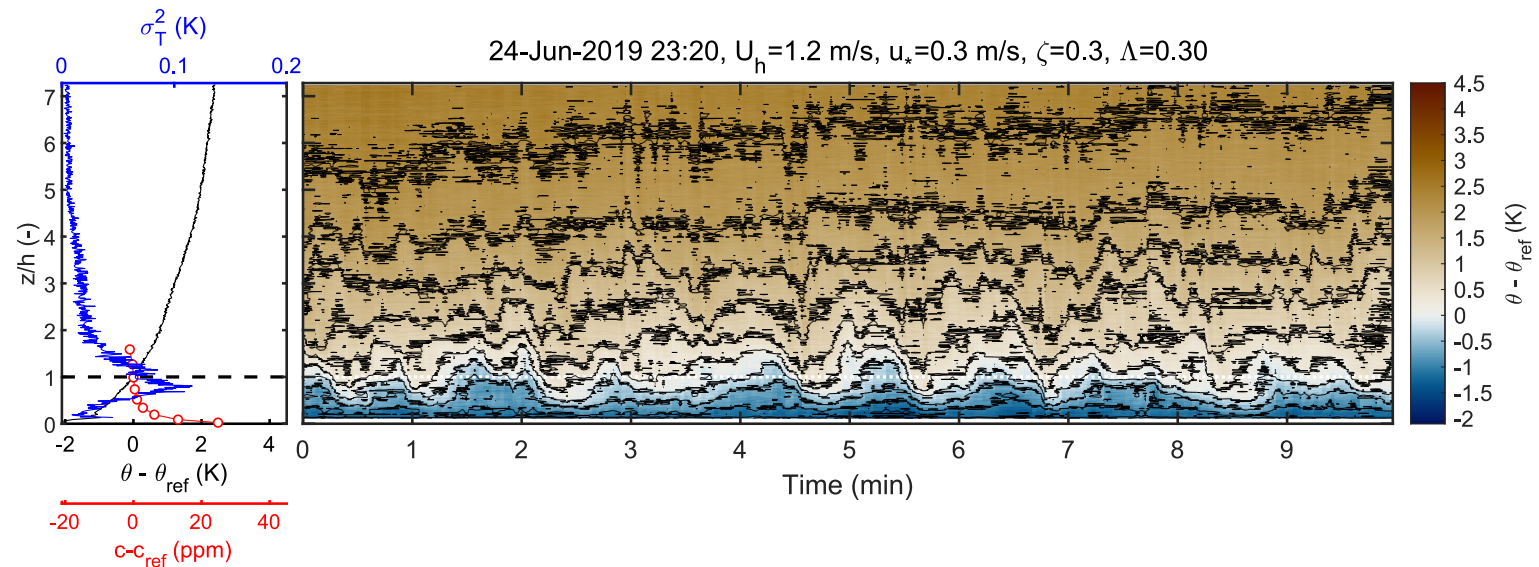


Figure 2.

a) quiescent, decoupled



b) turbulent above-canopy, decoupled



c) turbulent above- and below-canopy, coupled

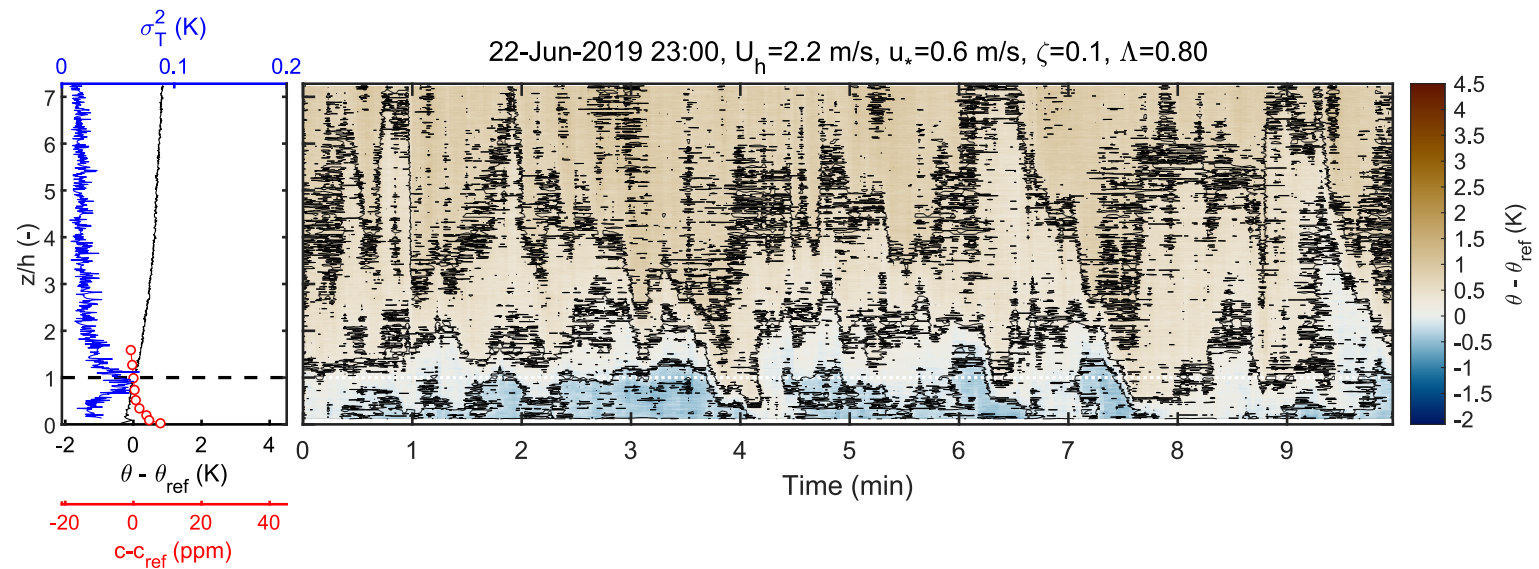
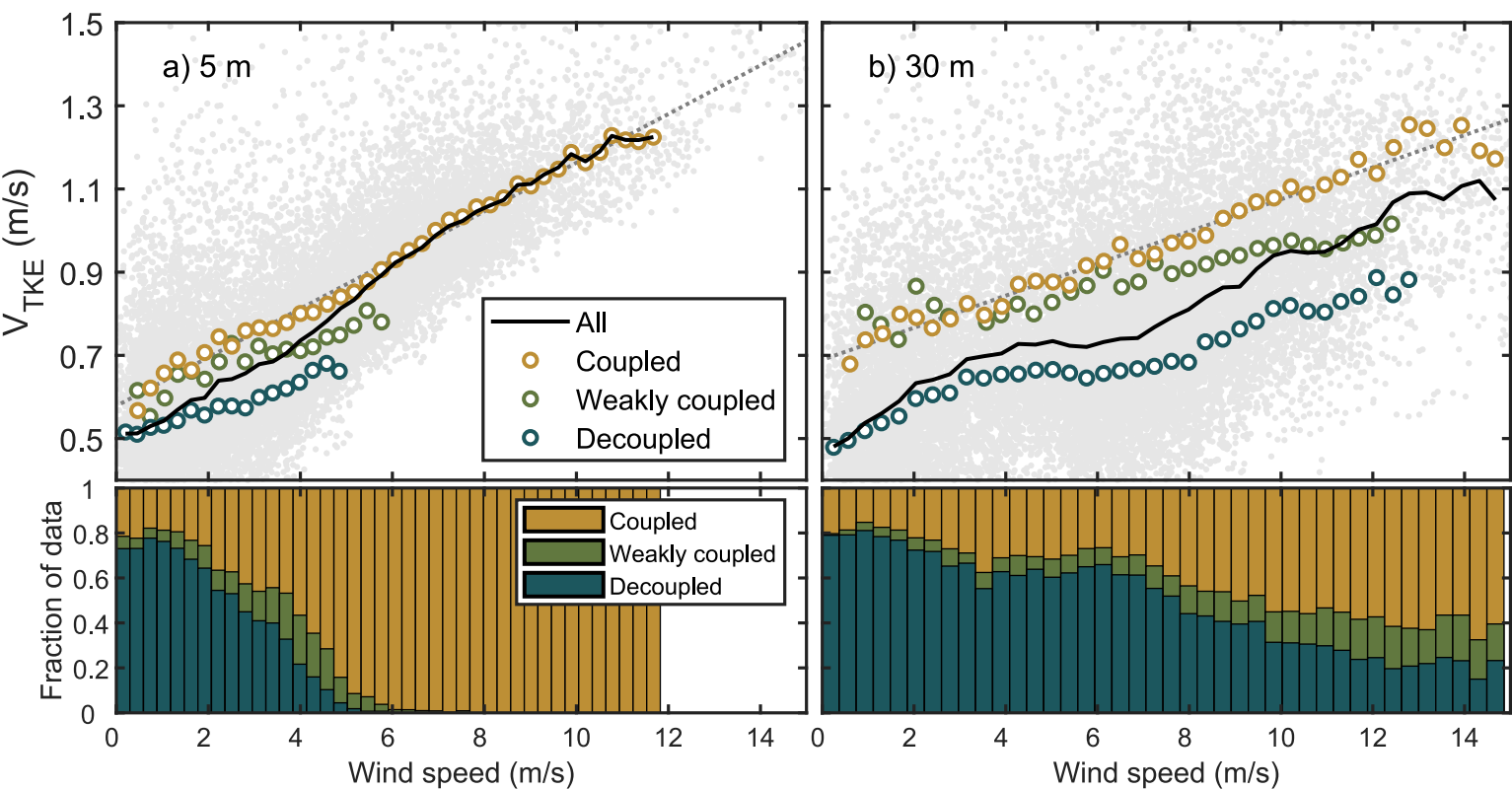


Figure 3.

Open flat terrain (FLOSS-II)



Boreal pine forest (Hyttiälä)

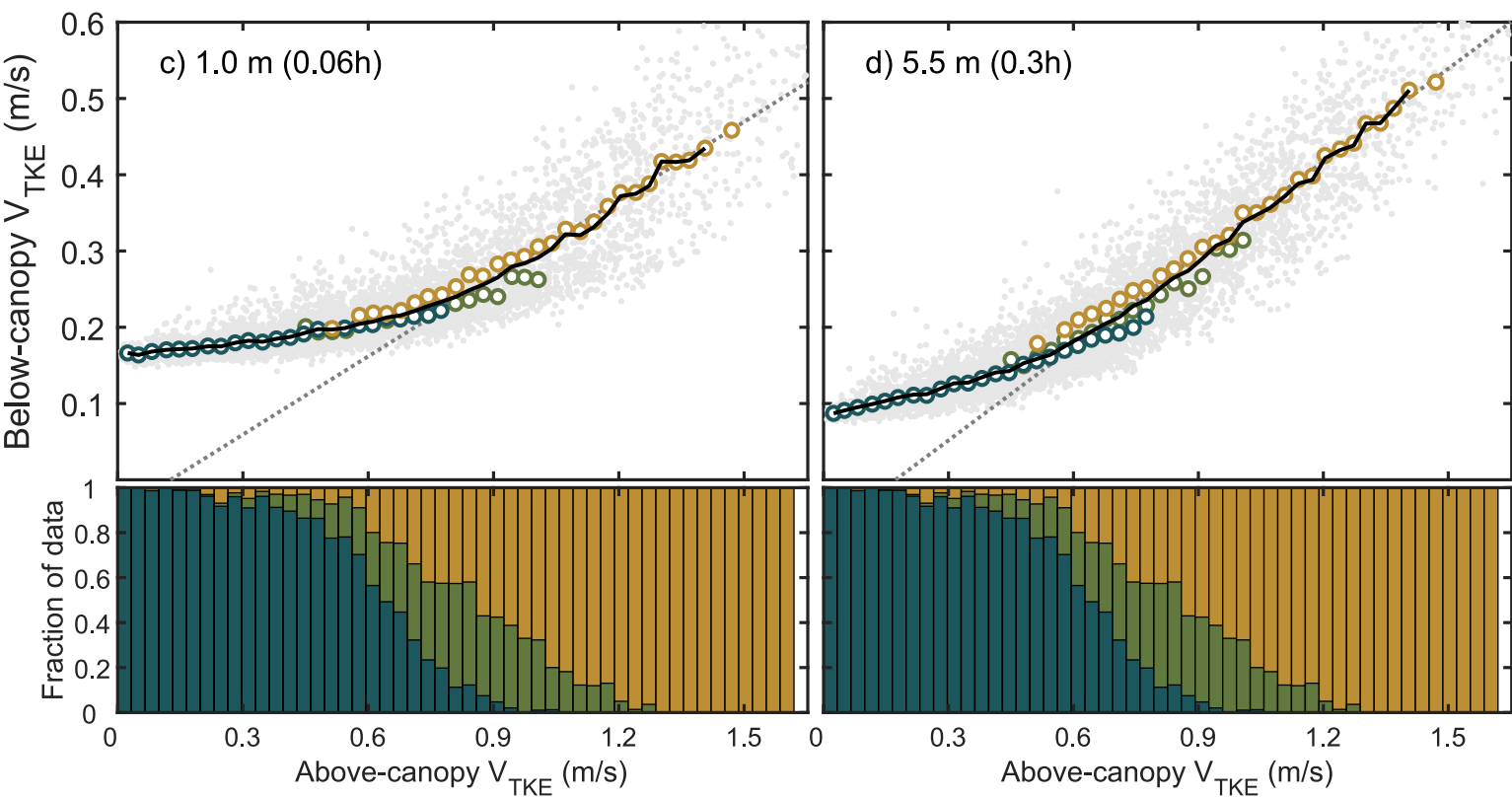
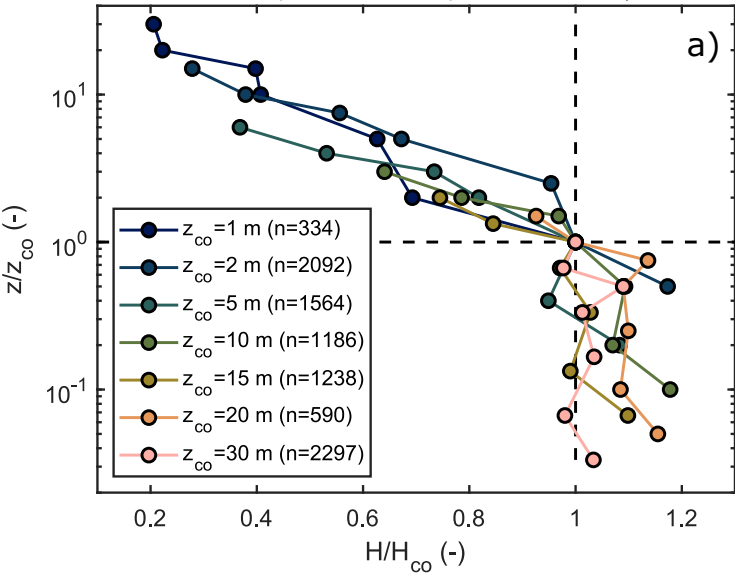


Figure 4.

Nocturnal H flux profile above open flat terrain (FLOSS-II)

Nocturnal CO₂ fluxes above boreal pine forest (Hyttiälä)